ACS Sustainable Chemistry & Engineering

Research Article

pubs.acs.org/journal/ascecg

Interaction of Ionic Liquid [bmin][CF_3SO_3] with Lysozyme Investigated by Two-Dimensional Fourier Transform Infrared Spectroscopy

Kun Du,[†] Jian Sun,[†] Xiaoqiang Song,[†] Huaming Chen,[†] Wei Feng,*[,†] and Peijun Ji*[,‡]

[†]Beijing Key Lab of Bioprocess, Department of Biochemical Engineering, Beijing University of Chemical Technology, Beijing 100029, China

[‡]Department of Chemical Engineering, Beijing University of Chemical Technology, Beijing 100029, China

ABSTRACT: The combination of ionic liquids with lysozyme has a potential application in food processing and analysis. In this work, at acid conditions, the interaction mechanism of the ionic liquid 1-butyl-3-methylimidazolium trifluoromethansulfonate with lysozyme has been investigated by two-dimensional Fourier transform infrared spectroscopy (FTIR). The residues and structures of lysozyme that have preferential interactions with the ionic liquid have been identified. The interaction mechanism can explain experimental results at acidic conditions where it was found that the presence of the ionic liquid is positively correlated to the enhanced enzymatic activity of the hen egg white lysozyme.

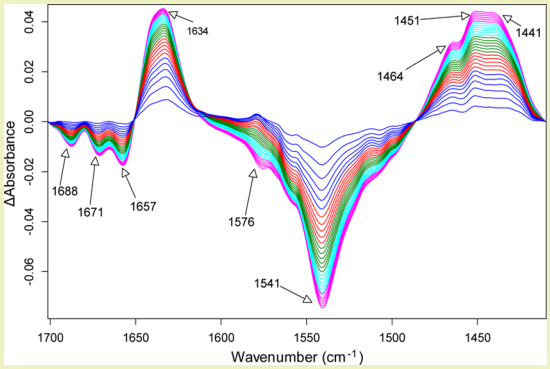

KEYWORDS: *Ionic liquid, Lysozyme, Two-dimensional FTIR spectra, Interaction mechanism*

INTRODUCTION

Lysozyme is found in many natural systems. Hen egg whites are the raw materials of choice for the industrial-scale production of lysozyme. Lysozyme has been used to preserve fresh vegetables, fish, meat, and fruit.[1,2] Lysozyme inhibits the growth of deleterious organisms, thus prolonging shelf life.[3] Oysters, shrimp, and other sea foods can be preserved in refrigerated storage by treatment with aqueous solutions of lysozyme and NaCl.[1] The antimicrobial spectrum of lysozyme can be enhanced when it is used with other substances, such as disodium pyrophosphate and pentasodium tripolyphosphate.[4] Ionic liquids (ILs) comprising a cation and an anion[5] have been studied for dissolving banana pulps[6] and determining metals and organic compounds in food samples of different natures.[7−11] An array of quartz crystals coated with different room-temperature ionic liquids is proposed for the analysis of food flavors by quartz crystal microbalance measurements.[12] Various food stuffs were solubilized in ionic liquids for rapid detection and quantification of bacterial pathogens.[13] Using an ionic liquid-containing system to perform simultaneous analysis for multiple contaminants fosters a more effective mode of operation in food control routines.[14] The combination of ionic liquids with lysozyme has a potential application in food processing and analysis.

The physical and chemical properties of ionic liquids can be tuned by systematically varying the cation−anion combination.[15] For taking this advantage in an enzymatic process, understanding of the effect of ILs on the conformational change of enzymes is essential. Circular dichroism spectroscopy has been widely used for examining secondary structure and conformational changes of proteins involving ionic liquids.[16−18] However, the specific interactions between enzymes and ILs and the dynamic structural change of the enzymes still remain to be demonstrated. Fourier transform infrared spectroscopy is often employed as a complementary method to elucidate functionally related environmental effects on protein structures.[16,19−22] The method of two-dimensional infrared spectroscopy is providing new approaches that can be used for visualizing conformational dynamics and characterizing conformational variation and structural disorder.[23−26] Probing the mechanism of enzyme structural changes are dynamics experiments that characterize structure during its evolution along a reaction coordinate.[23] Two-dimensional infrared spectroscopy can support the dynamic changes of the enzymes submitted to external perturbations due to chemical and physical factors.[23−26]

Considering the high number of enzymes and the significant combination of anions and cations that could compose an ionic liquid, a general and efficient methodology to evaluate the influence of an ionic liquid on a protein structure is necessary. This work aims to dynamically investigate structural changes of a model enzyme lysozyme upon interaction with ionic liquid in aqueous solutions. The conformational behavior and transient molecular structure and dynamics of lysozyme in the ionic

Received: December 15, 2013
Revised: April 18, 2014
Published: April 23, 2014

liquid solution have been studied by two-dimensional infrared (2D IR) spectroscopy. The results of FTIR spectra are correlated with the enzyme activity in the ionic liquid solution. The methodology can be extended to other enzymes/proteins interacting with ionic liquids.

METHODOLOGY

Thrice crystallized, dialyzed, and lyophilized hen egg white lysozyme, *Micrococcus lysodeikticus*, dipotassium deuterium phosphate, and potassium dideuterium phosphate were purchased from Sigma-Aldrich (Shanghai, China). D_2O was purchased from Merck (Germany). 1-Butyl-3-methylimidazolium trifluoromethansulfonate (HPLC purity >99%) was obtained from the Institute of Process Engineering, Chinese Academy of Sciences (Beijing, China).

The activity of lysozyme was measured using spectrophotometric turbidity assay. The lysozyme was dissolved into 66 mM potassium phosphate buffer (pH 6.23 and pH 5.0) in vials; the ionic liquid was added and shaken at 150 rpm at 35 °C. The concentrations of lysozyme and ionic liquid were 0.1 mg/mL and 0.003 M, respectively. A stock substrate solution of *Micrococcus lysodeikticus* was prepared in 66 mM potassium phosphate buffer with a concentration of 0.3 mg/mL. A portion (0.3 mL) of the lysozyme solution was mixed with 2.5 mL of *Micrococcus lysodeikticus* substrate into a cuvette. The change in absorbance at 450 nm, which reflects the hydrolysis of the cell wall substrate, was measured using a Shimadzu UV−vis 2500 spectrophotometer at 35 °C. The average values were based on triplicate measurements.

For dynamically measuring FTIR spectra of the lysozyme interacting with the ionic liquid, the ionic liquid must be pretreated by performing hydrogen−deuterium exchange experiments. The incubation of the ionic liquid (2 mL) with D_2O (5 mL) was performed for 3 days at room temperature, and then the ionic liquid was freeze-dried. The incubation of the freeze-dried ionic liquid with D_2O was performed for another 4 days at room temperature. The deuteration of the ionic liquid was monitored by measuring FTIR spectrum dynamically. It was found that the hydrogen−deuterium exchange for 7 days is enough for deuterating ionic liquid. The finally deuterated ionic liquid was dried under vacuum at 70 °C and then kept tightly sealed to minimize absorption of atmospheric moisture.

Infrared spectra were recorded on a Bruker Tensor 27 FTIR spectrometer equipped with a liquid nitrogen-cooled MCT detector at a nominal resolution of 2 cm^{-1}. Each spectrum is the result of the accumulation and averaging of 512 interferograms. The sample compartment was continuously purged with ultrapure nitrogen to minimize the spectral contribution of atmospheric water. The sample was filled into AquaSpec cell via an injection port. The AquaSpec cell is a flow-through transmission cell, with a path length of about 7 μm. The windows of the cell are made of CaF2. The cell is integral part of CONFOCHECK, a FTIR system that is specially designed for protein analysis. The temperature (35 °C) of the sample cuvette was controlled by a thermostat.

Lysozyme was dissolved in 66 mM deuterated potassium phosphate buffer (pD 5.0 and 6.23) with a concentration of 30 mg/mL, and then the deuterated ionic liquid, with a concentration of 0.897 M, was added into the lysozyme solution. The samples were rapidly prepared at 10 °C to avoid condensation of atmospheric water into the samples. D_2O was added into the lysozyme solution. The hydrogen−deuterium exchange experiment was carried out for 10 h. The pure spectra of lysozyme were obtained by subtracting the spectra of D_2O, and the ionic liquid was recorded under identical conditions.

Tertiary structural change of the lysozyme interacting with the ionic liquid was monitored by measuring fluorescence spectra. All measurements were carried out on a F-7000 spectrofluorimeter. The slits are 5 nm for excitation and emission scans. The measurement was carried out by excitation at 230 nm at the PMT voltage of 700 V. The scan speed was kept at 1200 nm/min, and the emission spectra were collected from 200 to 500 nm. The concentration of lysozyme was 10 μM, and the concentrations of ionic liquid were 0, 0.5, 1.0, 1.5, 2.0, 2.5, and 3.0 mM. The measurements were performed at 35 0C.

RESULTS

Enzymatic Activity of Lysozyme in the Presence of Ionic Liquid. Lysozyme may be utilized at various pH conditions. However, pH conditions have an effect on the activity of lysozyme. For example, with the difference of only 1.2 pH, the activity at pH 5.0 retains about 70% of that at pH 6.23 (optimal). The small difference of pH has caused a large difference between the activities, so the systems at pH 5.0 and 6.23 have been chosen for the investigations. A water-soluble ionic liquid 1-butyl-3-methylimidazolium trifluoromethansulfonate was tested to recover lysozyme activity at pH 5.0. When adding this ionic liquid to the solutions, the lysozyme activity at pH 5.0 is slightly lower than that at pH 6.23 as illustrated in Figure 1, demonstrating that the activity at pH 5.0 is recovered

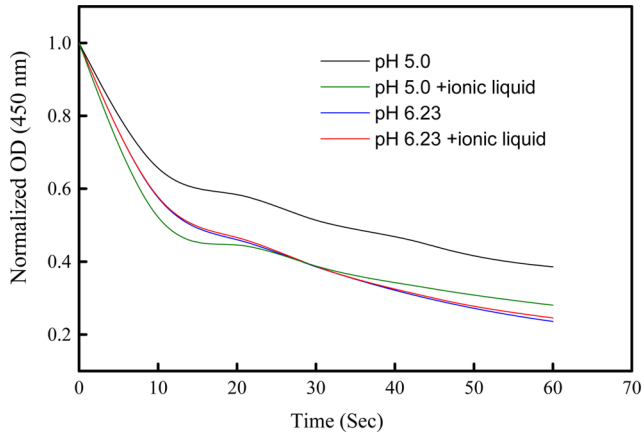

Figure 1. Turbidimetric assay of lysozyme in solution against *M. lysodeikticus*.

in the presence of the ionic liquid. To investigate the mechanism behind this phenomenon, fluorescence spectroscopy and two-dimensional Fourier transform infrared spectroscopy have been applied as the tools.

Fluorescence Spectra. The systems were investigated by fluorescence spectroscopy. The quenching of the intrinsic fluorescence of lysozyme by the ionic liquid was investigated to get information on the interactions between the ionic liquid and protein. Figure 2 shows the fluorescence spectra of lysozyme in the presence of the ionic liquid with excitation of 230 nm. It is shown that the intensity of the fluorescence spectra was reduced with the addition of the ionic liquid. It was suggested that the ionic liquid molecule interacted with the tryptophanyl residues of lysozyme causing the loss of the fluorescence (quenching).[27] In the present investigations, the fluorescence intensity arisen from the tested ionic liquid at 340 nm with excitation at 230 nm is significantly lower than that of lysozyme obtained at the same conditions. This is consistent with that reported in the previous literature; ionic liquids are found to exhibit a very low fluorescence efficiency.[28]

The quenching exhibits a concentration-dependence that can be described by the Stern−Volmer equation.[29]

$$\frac{F_0}{F} = 1 + K_{sv}[Q]$$

F_0 and F stand for the fluorescence intensities in the absence and presence of the quencher with a concentration of [Q], respectively, K_{SV} is the Stern−Volmer quenching constant.

dx.doi.org/10.1021/sc500218e | ACS Sustainable Chem. Eng. 2014, 2, 1420−1428

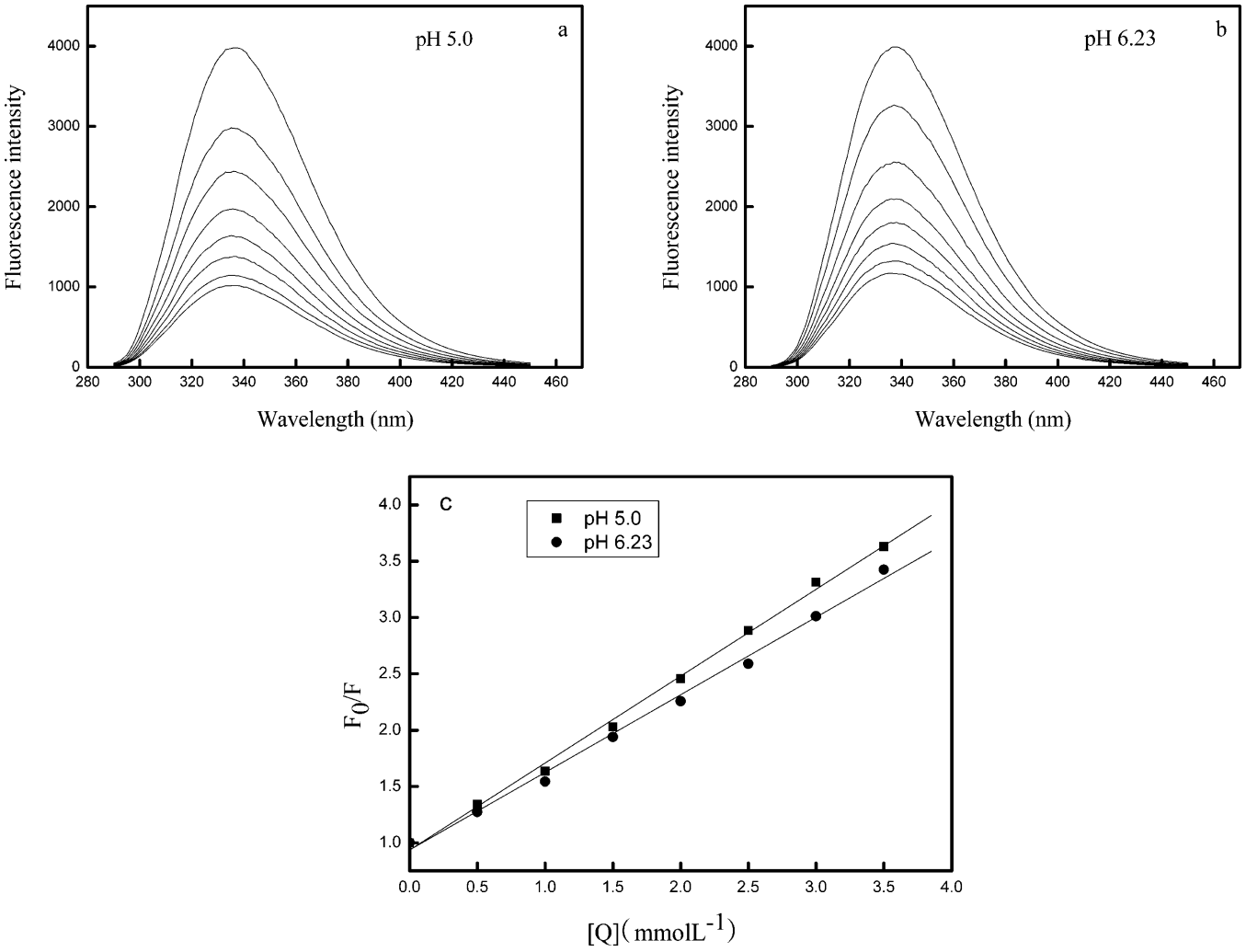

Figure 2. Fluorescence emission spectra with different concentrations of the ionic liquid in (a) and (b). Concentrations of the ionic liquid from top to bottom: 0, 0.5, 1.0, 1.5, 2.0, 2.5, and 3.0 mM. (c) Stern−Volmer plots for the quenching of lysozyme fluorescence by the ionic liquid.

As generally accepted, conformational changes can be investigated by comparing KSV constant.[30] Figure 2a and b show that with the increase in the concentration of ionic liquid, the fluorescence intensities are decreased, indicating the interactions of the ionic liquid with the lysozyme. Figure 2c represents the Stern−Volmer plots for the lysozyme at different concentrations of the ionic liquid. The KSV value of the lysozyme at pH 5.0 (0.7721) is slightly larger than that at pH 6.23 (0.6888), indicating that in the presence of the ionic liquid the conformation of the lysozyme at pH 5.0 has not been changed significantly compared to that at pH 6.23. This is in accordance with the result of enzymatic activity (Figure 1). To further investigate the interaction of lysozyme and the ionic liquid, FTIR spectra have been measured and analyzed.

FTIR Spectra Measured by Deuteration of Lysozyme at pD 6.23. Hen egg white lysozyme is a small monomeric protein of 129 residues.[1,2] It has two structural domains. The alpha domain is composed of four α-helices and a 3_{10} helix. The beta domain is composed of a triple stranded antiparallel β-sheet, a 3_{10} helix, and a long loop. The active site contains the two catalytic residues, Glu 35 and Asp 52. Figure 3a shows a series of infrared spectra of lysozyme recorded as a function of the deuteration time at pD 6.23. As shown, upon H−D exchange, the intensity and position of the amide bands are affected. The most intense absorption band occurs near 1660 cm^{-1} and is due to the amide I vibration.[23] This vibration involves mostly the stretching of the amide C═O group.[23,31] The amide II band around 1548 cm^{-1} is mainly due to the in-plane N−H bending vibration coupled with the C−N stretching vibration of the peptide bond.[31] During the deuteration process, the intensity of the amide II band (1548 cm^{-1}) decreases, while that of the amide II′ band (1454 cm^{-1}) increases.

Figure 3b shows the difference spectra as a function of deuteration time, which were obtained by subtracting from each spectrum of Figure 3a the spectrum recorded just before the beginning of the deuteration process. The spectral changes occurring upon H−D exchange are clearly shown in Figure 3b. The changes arise from the amide I and II vibrations of the different secondary structures as well as the vibrations of the side chains of residues.[23] The negative band with minima at 1692 cm^{-1} is assigned to the decrease in the intensity of the amide I bands of amide groups involved in β-sheets.[32,33] The negative bands at 1674/1662 and 1548 cm^{-1} are assigned to the β-turn and α-helix structures, respectively.[34−38] The small shoulder at 1538 cm^{-1} is assigned to the β-sheet.[36] The small shoulder observed at 1516 cm^{-1} on the negative amide II band is due to the deuteration of the single tyrosine residue of

dx.doi.org/10.1021/sc500218e | ACS Sustainable Chem. Eng. 2014, 2, 1420−1428

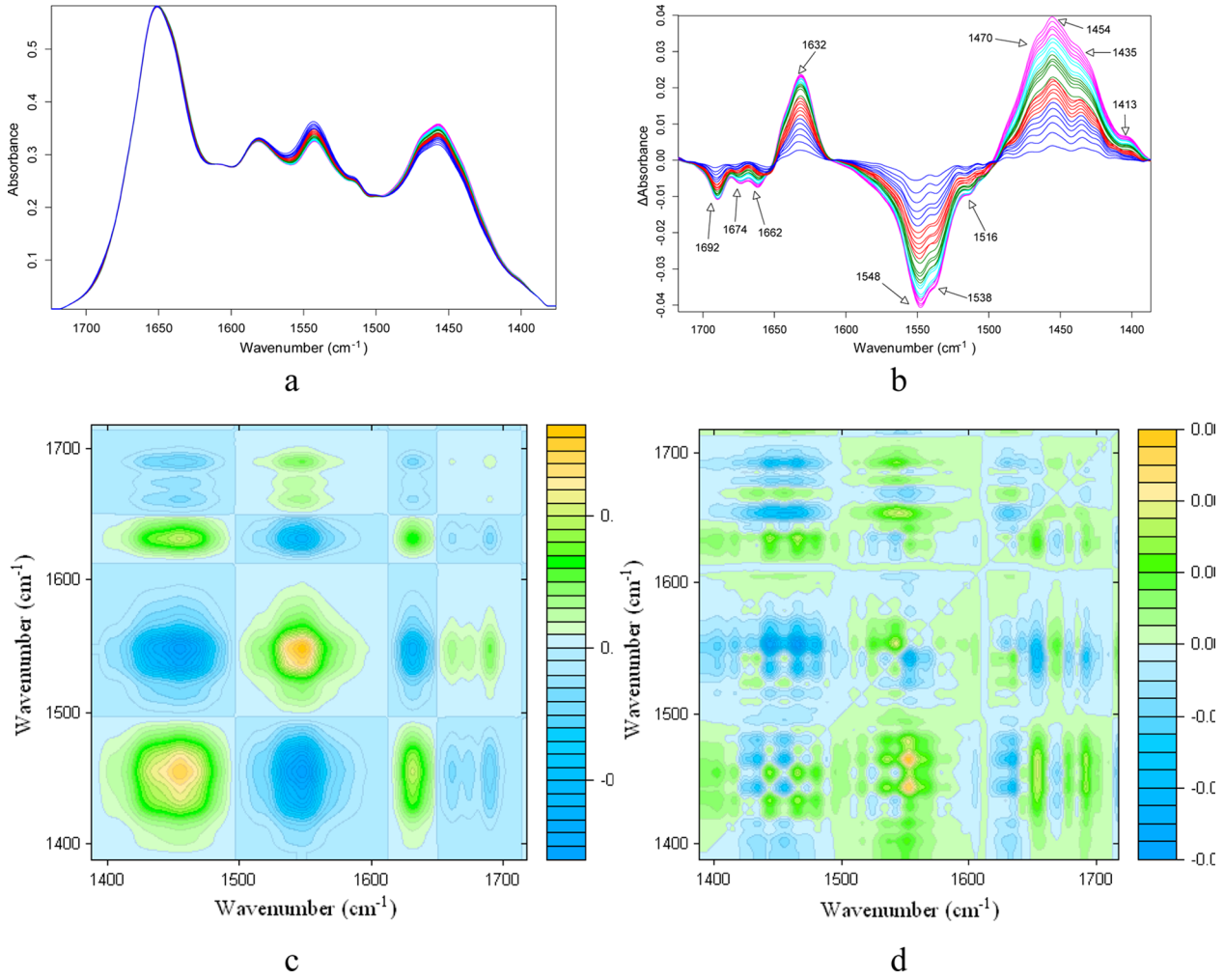

Figure 3. Infrared spectra (a) and difference spectra (b) of lysozyme as a function of the deuteration time. Synchronous (c) and asynchronous (d) 2D correlation spectra of lysozyme obtained for 90 min of deuteration. pD 6.23. In spectra (a) and (b), the deuteration time was increased from the lines in blue to the lines in pink.

lysozyme.[32] The positive bands at 1632 and 1454 cm^{-1} are assigned to the β-sheet of the amide I′ vibration and unordered loop of the amide II vibration, respectively.[34−38] The small shoulders at 1470 and 1435 cm^{-1} are due to the unordered loop and α-helix structures, respectively.[23]

The synchronous and the asynchronous correlation maps were obtained as presented in Figure 3c and d. On the synchronous map, the diagonal elements (autopeaks) represent the variance of spectral signal fluctuations as a function of time for the representative spectral variable, while the cross-peaks correspond to the covariance between spectral signal fluctuations at two separated spectral variables.[26] The relative direction between the spectral variations can be determined by the sign of the cross-peaks. A positive cross-peak implies that the intensity variations are changing in a similar way (the intensity of two bands increases or decreases simultaneously), while a negative cross-peak means that the intensity variations are changing in opposite directions (one band increases in intensity while the other one decreases).[23] The strongest autopeak at 1454 cm^{-1} is due to the increasing magnitude of the amide II′ band, while the relatively weak peak at 1548 cm^{-1} corresponds to the decreasing magnitude of the amide II signal.[38] The negative cross-peaks observed at 1548 and 1454 cm^{-1} are due to the fact that the amide II band at 1548 cm^{-1} is replaced by the amide II′ band at 1454 cm^{-1} upon deuteration of the amide protons.[23,34,38] However, the synchronous map in the amide II and amide II′ region does not display a clearly resolved spectral contribution for the different conformations present in the protein. The synchronous and asynchronous correlation spectra are powerful tools for the deconvolution of overlapping vibrational bands and enable a more critical analysis of the order of exchange for the same or different secondary structural elements.[15,26,31] An asynchronous cross-peak develops only if the intensities of two spectral features change out of phase (i.e., delayed or accelerated) with each other. A cross-peak is observed if the change is faster or slower relative to the corresponding spectral coordinates. By combining the sign of the peaks in the synchronous and asynchronous maps, the sequence of the spectral variations can be determined.[23] The main correlation peaks observed in the asynchronous map of Figure 3d are summarized in Table 1. The band assignment is based on the existing literature on infrared spectroscopy of proteins,[23−26,31−39] and the sequential order of exchange along the time axis is determined from Noda's rules.[40]

Band assignments and Noda's rules confirm that the β-sheet structure (1630 cm^{-1}) exchanges before the α-helix structure (1653 cm^{-1}). This sequence is also confirmed by the cross-peak

dx.doi.org/10.1021/sc500218e | ACS Sustainable Chem. Eng. 2014, 2, 1420−1428

Table 1. Assignment of Cross-Peaks Found on Asynchronous Correlation Maps of Figures 2d and 3c

pD 6.23		pD 5.0	
faster exchanging component (cm^{-1})[a]	slower exchanging component (cm^{-1})[a]	faster exchanging component (cm^{-1})[a]	slower exchanging component (cm^{-1})[a]
1667 (t)	1653 (α)	1475 (Asp)	1430 (α)
1669 (t)	1692 (β)	1509 (Tyr)	1456 (u)
1669 (t)	1678 (β)	1460 (u)	1544 (α)
1686 (Gln)	1653 (α)	1600 (Arg)	1455 (u)
1669 (t)	1634 (β)	1585 (Arg)	1545 (α)
1630 (β)	1653 (α)	1460 (u)	1630 (β)
1642 (u)	1653 (α)	1550 (α)	1630 (β)
1542 (u)	1678 (β)	1550 (α)	1640 (β)
1669 (t)	1553 (α)	1465 (u)	1654(α)
1642 (u)	1553 (α)	1595 (Arg)	1654 (α)
1542 (u)	1634 (β)	1602 (Arg)	1631 (β)
1605 (Arg)	1550 (α)	1650 (α)	1632 (β)
1669 (t)	1455 (u)	1662 (t)	1632 (β)
1460 (u)	1653 (α)	1654 (α)	1666 (β)
1542 (u)	1534 (β)	1460 (u)	1687 (β)
1525 (β)	1553 (α)	1585 (Arg)	1688 (β)

[a]The band assignment is based on refs 23−26 and 31−39. α: α-helix. β: β-sheet. t: β-turn. u: unordered structure.

at 1525 vs 1553 cm^{-1}. The presence of hydrogen bonds in α-helices explains why the deuteration is slower than for the β-sheet structure. Similarly, the existence of the 1669 vs 1634 cm^{-1} and 1642 vs 1653 cm^{-1} cross-peaks suggests that the turn structure exchanges before the β-sheet structure and the unordered structure exchanges before the α-helix structure. Additional cross-peaks are observed at 1542 vs 1634 cm^{-1} and 1669 vs 1445 cm^{-1}, suggesting that the unordered structure exchanges before the β-sheet structure and the turn structure exchanges before the unordered structure. β-Sheet protons are more difficult to exchange than those of irregular structures because of the presence of strong hydrogen bonds in β-sheets. The absence of regular hydrogen bonds of the unordered structure most likely allows the amide protons to be exchanged more easily than those of α-helices and β-sheets. In the tertiary structure of lysozyme shown in Figure 1, most of the glutamine and arginine residues are found on the outer surface of the lysozyme molecule.[32] The accessibility of the side chain protons can explain why they are rapidly exchanged, as suggested by the cross-peaks at 1686 and 1653 cm^{-1} and 1605 and 1550 cm^{-1}. From these results, we can therefore conclude that the relative order of deuteration of the lysozyme protons is as follows: Gln, Arg, turns > unordered structure > β-sheet > α-helices.

FTIR Spectra Measured by Deuteration of Lysozyme at pD 5.0. Figure 4a presents difference spectra as a function of deuteration time. The negative band at 1654 cm^{-1} is assigned to the α-helix structure; the positive band at 1463 cm^{-1} is for the unordered structure. Figure 4b and c present the synchronous and the asynchronous correlation maps, and the sequence of deuteration of the different peaks are summarized in Table 1. It can be concluded that turns and side chains of Arg and Asp are the first elements to be deuterated. The characteristic wavenumber position of turns is 1662 cm^{-1} in the amide I region; 1585, 1600, and 1602 cm^{-1} are due to the side chains of arginine residue.[32] In the tertiary structure of lysozyme as shown in Figure 1, turns and most of the arginine residues are found on the outer surface of the lysozyme

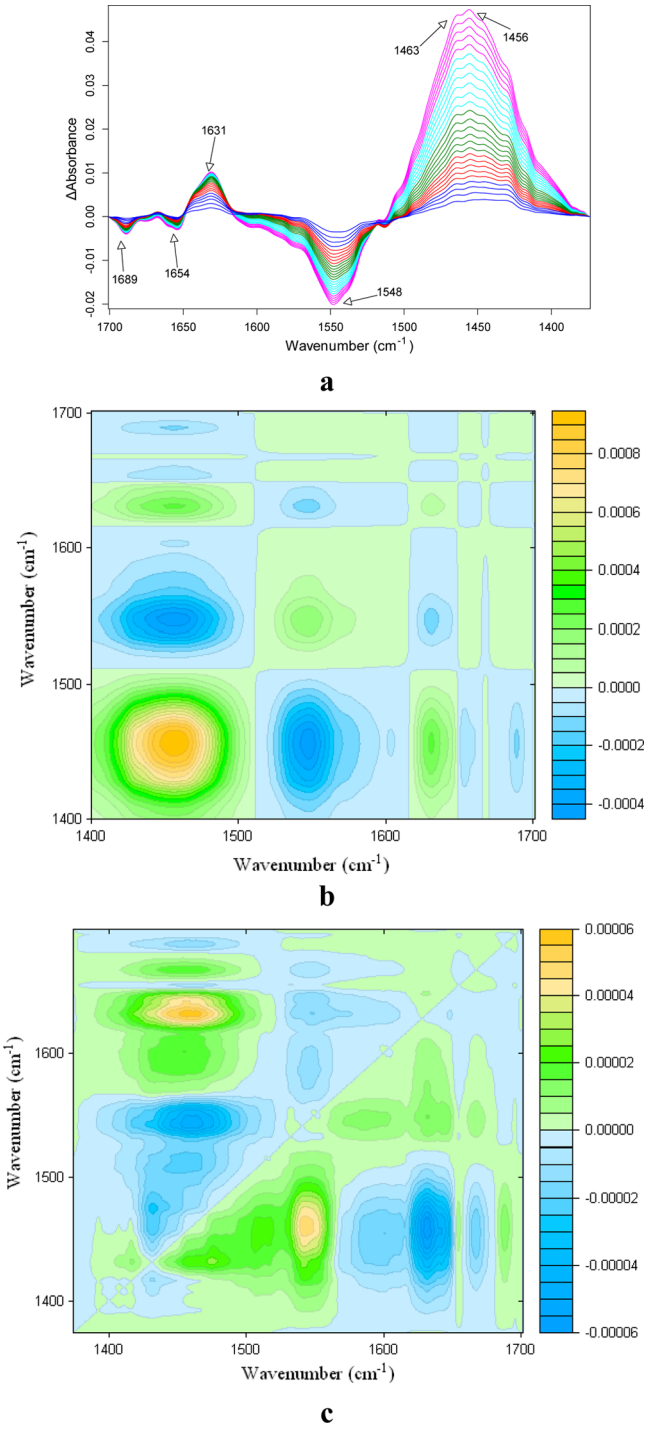

Figure 4. Difference spectra (a) of lysozyme as a function of the deuteration time. Synchronous (b) and asynchronous (c) 2D correlation spectra of lysozyme obtained for 90 min of deuteration. pD 5.0. In the spectra (a), the deuteration time was increased from the lines in blue to the lines in pink.

molecule.[32] The accessibility of these amide and side chain protons can explain why they are rapidly exchanged. The unordered structure is the next one to be deuterated, and its characteristic wavenumbers are 1460 and 1465 cm^{-1}. The α-helix is the third secondary structure to be deuterated. The wavenumber positions associated with this structure are 1430, 1545, 1550, 1650, and 1654 cm^{-1}.[31,39] The latest protons to be exchanged during the initial deuteration period are those of the

dx.doi.org/10.1021/sc500218e | ACS Sustainable Chem. Eng. 2014, 2, 1420−1428

backbone of the β-sheets in the amide I region (1630, 1640, 1666, 1688 cm^{-1}).

The H−D change of the α-helices is faster than that of the β-sheets. This implies that there is a conformational change when altering the pD from pD 6.23 (optimal) to pD 5.0. This is consistent with the lytic activity toward *Micrococcus lysodeikticus* cell walls. The lytic activity at pH 5.0 is much reduced as compared to that at pH 6.23. The charge on individual residues will alter depending on the pH condition. For example, the pK_a of His-15 is 5.36 ± 0.07.[41] At pH 6.23, His-15 is deprotonated; while at pH 5.0, it is protonated.[42−44] The pK_a for Glu-35 of hen egg white lysozyme is 6.2 ± 0.1.[41] At pH 6.23, occurrence of deprotonated Glu-35 is possible; while at pH 5.0, Glu 35 is protonated. Both Glu35 and His15 are in α-helices. His15 of hen egg white lysozyme is remote from the active site[45,46] The protonation state of His-15 does not seem to play a direct role in controlling the lytic activity toward *M. lysodeikticus* cell walls.[46,47] The decreased lytic activity observed at pH 5.0 is related reasonably to the protonation state of Glu-35, which is involved in the activity of lysozyme. The hydrogen bond networks are very important in active sites.[48] As pH changes, hydrogen bonds will be broken and reformed elsewhere to reflect their protonation state. Possibly, this is one of the reasons for the conformational change of the lysozyme at pH 5.0. In addition, decreasing the pH increases the likelihood of protonating a side chain group, and consequently, electrostatic interactions between two residues are changed.

FTIR Spectra Measured by Deuteration of Lysozyme in the Presence of Ionic Liquid at pD 6.23. Figure 5a shows a series of difference spectra recorded as a function of the deuteration time in the presence of the ionic liquid at pD 6.23. The negative band with minima at 1688 cm^{-1} is assigned to the decrease in the intensity of the amide I bands of amide groups involved in β-sheets. The decreases in the intensity of bands at 1671, 1657, and 1541 cm^{-1} are due to the β-turn, α-helix, and unordered structures, respectively. The small shoulder observed at 1576 cm^{-1} on the negative amide II band is due to the deuteration of the Asp residue of lysozyme.[41] The positive bands at 1632 and 1441 cm^{-1} are assigned to β-sheet of the amide I′ vibration and unordered loop of the amide II′ vibration, respectively. The small shoulder at 1476 can be assigned to the Asp residue.

Figure 5b and c are for the synchronous and the asynchronous correlation maps, respectively. From the sequence of deuteration of the different peaks listed in Table 2, one can conclude that turns and side chains of Asn, Glu, and Asp are the first elements to be deuterated. The β-sheet is deuterated before the α-helices, and the protons of the backbone of the α-helices are the latest protons to be exchanged. The deuteration sequence is similar to that based in Figure 3d. This means that the conformation of lysozyme has been well preserved in the presence of the ionic liquid at pD 6.23. This is consistent with the results of catalysis as shown in Figure 1, which indicates that at the optimal pH condition (pH 6.23), the catalysis is not affected by the ionic liquid.

The results in Table 2 also indicate the fact that the unordered structure is one of the last components to be deuterated, even though it is not involved in hydrogen bonds, suggesting that this part of the protein interacts with the ionic liquid. The electronic and electronic−hydrophilic interactions can occur between the ionic liquid and the residues of unordered structure. In addition, the side chains of the Arg residues (1608 cm^{-1}) are deuterated after the unordered

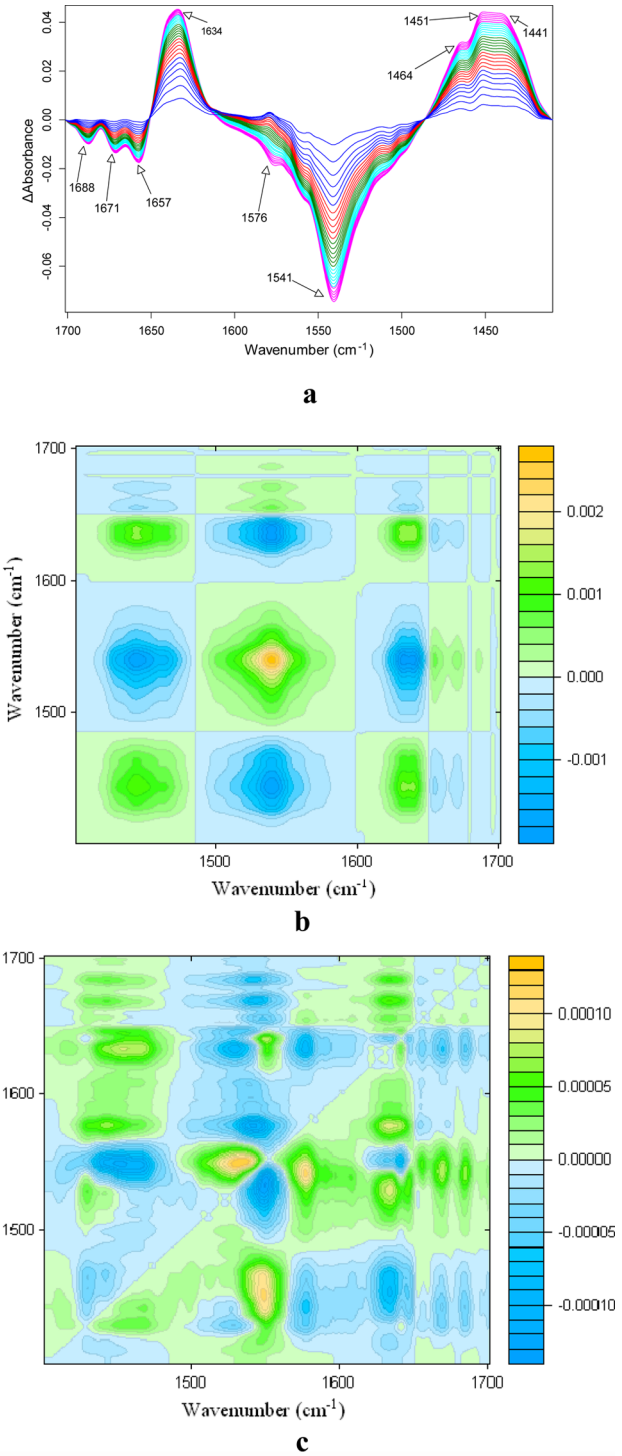

Figure 5. Difference spectra (a) of lysozyme as a function of the deuteration time. Synchronous (b) and asynchronous (c) 2D correlation spectra of lysozyme obtained for 90 min of deuteration. pD 6.23, in the presence of the ionic liquid. In the spectra (a), the deuteration time was increased from the lines in blue to the lines in pink.

structure (Table 2), suggesting that the ionic liquid with the anion (trifluoromethansulfonate) has a preferential interaction with the Arg residues.[49]

FTIR Spectra Measured by Deuteration of Lysozyme in the Presence of Ionic Liquid at pD 5.0. Figure 6a shows a series of difference spectra recorded as a function of the

dx.doi.org/10.1021/sc500218e | ACS Sustainable Chem. Eng. 2014, 2, 1420−1428

Table 2. Assignment of Cross-Peaks Found on Asynchronous Correlation Maps of Figures 4c and 6c

pD 6.23		pD 5.0	
faster exchanging component (cm^{-1})[a]	slower exchanging component (cm^{-1})[a]	faster exchanging component (cm^{-1})[a]	slower exchanging component (cm^{-1})[a]
1530 (β)	1550 (α)	1466 (u)	1544 (α)
1577 (Asp)	1444 (u)	1535 (β)	1548 (α)
1577 (Asp)	1542 (u)	1573 (Glu)	1545 (α)
1634 (β)	1518 (Tyr)	1470 (u)	1582 (Arg)
1641 (u)	1428 (α)	1468 (u)	1638 (β)
1454 (u)	1634 (β)	1630 (β)	1428 (α)
1641 (u)	1551 (α)	1635 (β)	1550 (α)
1578 (Asp)	1634 (β)	1573 (Glu)	1635 (β)
1668 (t)	1444 (u)	1664 (t)	1532 (β)
1684 (Asn)	1445 (u)	1525 (β)	1660 (α)
1669 (t)	1545 (α)	1573 Glu	1658 (α)
1685 (β)	1542 (α)	1635 (β)	1650 (α)
1578 (Asp)	1655 (α)	1669 (t)	1432 (α)
1669 (t)	1633 (β)	1682 (Asn)	1445 (u)
1685 (Asn)	1634 (β)	1669 (t)	1545 (α)
1688 (β)	1655 (α)	1683 (Asn)	1542 (u)
1684 (Asn)	1656 (α)	1683 (Asn)	1638 (β)
1682 (Asn)	1672 (t)	1669 (t)	1658 (α)
1541 (u)	1608 (Arg)	1683 (Asn)	1657 (α)

[a]The band assignment is based on refs 23−26 and 31−39. α: α−helix. β: β−sheet. t: β−turn. u: unordered structure.

deuteration time in the presence of the ionic liquid at pD 5.0. The difference spectra show the bands appearing with the deuteration time. Figure 6b and c shows the synchronous and the asynchronous correlation maps. The 2D asynchronous map (Figure 6c) shows that turns and side chains of Gln are the first elements to be deuterated. The β-sheet is deuterated before the α-helices, and the α-helices are the latest ones to be deuterated. The deuteration sequence at pD 5.0 is similar to that at pD 6.23, suggesting that there is no significant conformational changes of the lysozyme at pD 5.0 in the ionic liquid/D_2O solution. This is consistent with the lytic activity of lysozyme at pH 5.0 in the presence ionic liquid as illustrated in Figure 1. It indicated that the ionic liquid promotes the catalysis. Possibly, this is due to the buffering action as demonstrated by the ionic liquids in the aqueous mixture.[49] The results in Table 2 also indicate the fact that the unordered structure and Arg residues are the slower exchange components, suggesting their preferential interactions with the ionic liquid.

CONCLUSIONS

On the basis of the 2D IR correlation spectroscopy with hydrogen−deuterium exchange as the external perturbation, the structure of lysozyme in the absence and presence of ionic liquid has been investigated, and the chronological sequence of the deuteration of the different conformations and of some of the side chains was determined. The analysis of the 2D IR correlation spectra indicated that the ionic liquid interacts preferentially with the arginine residues and the unordered structures of the lysozyme. As most of the arginine residues are placed on the outer surface and the unordered structure is remote from the active site, the interactions have little effect on the activity site. As ionic liquids have been investigated for their utilization in food processing and analysis, ionic liquids can potentially be used for food preservation in combination with lysozyme. The increased knowledge of the effect of ionic liquid on lysozyme activity will be helpful for choosing ionic liquids

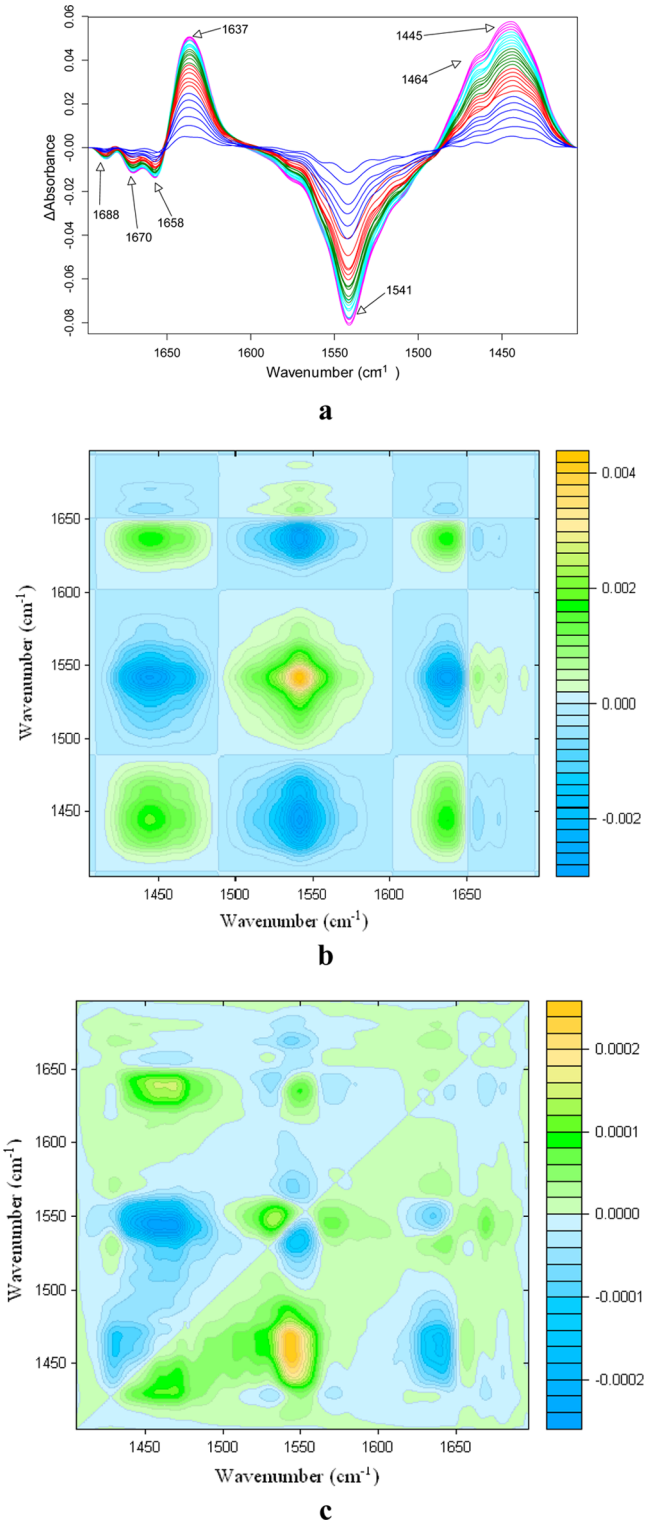

Figure 6. Difference spectra (a) of lysozyme as a function of the deuteration time. Synchronous (b) and asynchronous (c) 2D correlation spectra of lysozyme obtained for 90 min of deuteration. pD 5.0, in the presence of the ionic liquid. In the spectra (a), the deuteration time was increased from the lines in blue to the lines in pink.

dx.doi.org/10.1021/sc500218e | ACS Sustainable Chem. Eng. 2014, 2, 1420−1428

that can promote lysozyme activity in various conditions, which may be encountered in food storage and preservation.

AUTHOR INFORMATION

Corresponding Authors

*Tel.: +86-10-64446249. E-mail: fengwei@mail.buct.edu.cn (W.F.).

*Tel.: +86-10-64446249. E-mail: jipj@mail.buct.edu.cn (P.J.).

Author Contributions

K.D. and J.S. contributed equally to this work

Notes

The authors declare no competing financial interest.

ACKNOWLEDGMENTS

This work was supported by the National Science Foundation of China (21376021, 21176025), National Hi-tech R&D Program (2014AA022003), and National Basic Research Program of China (2011CB200905).

REFERENCES

(1) Proctor, V. A.; Cunningham, F. E.; Fung, D. Y. C. The chemistry of lysozyme and its use as a food preservative and a pharmaceutical. *Crit. Rev. Food Sci. Nutr.* **1988**, *26* (4), 359−395.

(2) Hughey, V. L.; Wilger, P. A.; Johnson, E. A. Antibacterial activity of hen egg white lysozyme against *Listeria monocytogenes* Scott A in foods. *Appl. Environ. Microb.* **1989**, *55* (3), 631−638.

(3) Cunningham, F. E.; Proctor, V. A.; Goetsch, S. J. Egg-white lysozyme as a food preservative: an overview. *World Poultry Sci.* **1991**, *47* (2), 141−163.

(4) Boland, J. S.; Davidson, P. M.; Weiss, J. Enhanced inhibition of *Escherichia coli* O157:H7 by lysozyme and chelators. *J. Food Prot.* **2003**, *66*, 1783−1789.

(5) Pereiro, A. B.; Araújo, J. M. M.; Martinho, S.; Alves; Nunes, S.; Matias, A.; Duarte, C. M. M.; Rebelo, L. P. N.; Marrucho, I. M. Fluorinated ionic liquids: Properties and applications. *ACS Sustainable Chem. Eng.* **2013**, *1* (4), 427−439.

(6) Fort, D. A.; Swatloski, R. P.; Moyna, P.; Rogers, R. D.; Moyna, G. Use of ionic liquids in the study of fruit ripening by high-resolution ^{13}C NMR spectroscopy: 'green' solvents meet green bananas. *Chem. Commun.* **2006**, *7* (0), 714−716.

(7) Martýn-Calero, A.; Pino, V.; Afonso, A. M. Ionic liquids as a tool for determination of metals and organic compounds in food analysis. *Trends Anal. Chem.* **2011**, *30* (10), 1598−1619.

(8) Ruiz-Aceituno, L.; Carrero-Carralero, C.; Ramos, L.; Martinez-Castro, I.; Sanz, M. L. Development of a carbohydrate silylation method in ionic liquids for their gas chromatographic analysis. *Anal. Chim. Acta* **2013**, *787* (17), 87−92.

(9) Ping, J.; Wang, Y.; Wu, J.; Ying, Y.; Ji, F. Determination of ascorbic acid levels in food samples by using anionic liquid−carbon nanotube composite electrode. *Food Chem.* **2012**, *135* (2), 362−367.

(10) Ruiz-Aceituno, L.; Sanz, M. L.; Ramos, L. Use of ionic liquids in analytical sample preparation of organic compounds from food and environmental samples. *TrAC, Trends Anal. Chem.* **2013**, *43* (0), 121−145.

(11) Abdolmohammad-Zadeh, H.; Sadeghi, G. H. Combination of ionic liquid-based dispersive liquid−liquid micro-extraction with stopped-flow spectrofluorometry for the pre-concentration and determination of aluminum in natural waters, fruit juice and food samples. *Talanta* **2010**, *81* (3), 778−785.

(12) Toniolo, R.; Pizzariello, A.; Dossi, N.; Lorenzon, S.; Abollino, O.; Bontempelli, G. Room temperature ionic liquids as useful overlayers for estimating food quality from their odor analysis by quartz crystal microbalance measurements. *Anal. Chem.* **2013**, *85* (15), 7241−7247.

(13) Mester, P.; Wagner, M.; Rossmanith, P. Use of ionic liquid-based extraction for recovery of *Salmonella typhimurium* and *Listeria monocytogenes* from food matrices. *J. Food Prot.* **2010**, *73* (4), 680−687.

(14) Ho, Y. M.; Tsoi, Y. K.; Leung, K. S. Y. Ionic-liquid-based dispersive liquid−liquid microextraction for high-throughput multiple food contaminant screening. *J. Sep. Sci.* **2013**, *36* (23), 3791−3798.

(15) Chowdhury, S.; Mohan, R. S.; Scott, J. L. Reactivity of ionic liquids. *Tetrahedron* **2007**, *63* (11), 2363−2389.

(16) Morris, V. K.; Ren, Q.; Macindoe, I.; Kwan, A. H.; Byrne, N.; Sunde, M. Structural insights into differences in drug-binding selectivity between two forms of human alpha1-acid glycoprotein genetic variants, the A and F1*S forms. *J. Biol. Chem.* **2011**, *286* (16), 5955−15963.

(17) Diego, T. D.; Lozano, P. S.; Gmouh, M.; Vaultier, J.; Iborra, L. Fluorescence and CD spectroscopic analysis of the alpha-chymotrypsin stabilization by the ionic liquid,1-ethyl-3-methylimidazolium bis[(trifluoromethyl)sulfonyl]amide. *Biotechnol. Bioeng.* **2004**, *88* (7), 916−924.

(18) Zhang, Z.; Pan, W. Ionic liquids: Green solvents for nonaqueous biocatalysis. *Enzyme Microb. Technol.* **2005**, *37* (1), 19−28.

(19) Güler, G.; Dzafic, E.; Vorob'ev, M. M.; Vogel, V.; Mantele, W. Real time observationof proteolysis with Fourier transform infrared (FT-IR) and UV-circular dichroism spectroscopy: Watching a protease eat a protein. *Spectrochim. Acta, Part A* **2011**, *79* (1), 104−111.

(20) Yu, L.; Xiang, B. Two-dimensional near-IR correlations pectroscopy study the interaction of protein and famotidine in acidic pH region. *Spectrochim. Acta, Part A* **2008**, *69* (2), 599−603.

(21) Mecozzi, M.; Pietroletti, M.; Tornambè, A. Molecular and structural characteristics in toxic algae cultures of Ostreopsis ovata and Ostreopsis spp. evidenced by FTIR and FTNIR spectroscopy. *Spectrochim. Acta, Part A* **2011**, *78* (5), 1572−1580.

(22) Yu, P.; Jonkera, A.; Gruber, M. Molecular basis of protein structure in proanthocyanidinand anthocyanin-enhanced Lc-transgenic alfalfa in relation to nutritive value using synchrotron-radiation FTIR microspectroscopy: A novel approach. *Spectrochim. Acta, Part A* **2009**, *73* (5), 846−853.

(23) Richard, J. A.; Kelly, I.; Marion, D.; Auger, M.; Pezolet, S. M. Structure of β-purothionin in membranes: A two-dimensional infrared correlation spectroscopy study. *Biochemistry* **2005**, *44* (1), 52−61.

(24) Carmona, P.; Molina, M. Interactions of protein and nucleic acid components of hepatitis C virus as revealed by fourier transform infrared spectroscopy. *Biochemistry* **2010**, *49* (23), 4724−4731.

(25) Pechkova, E.; Innocenzi, P.; Malfatti, L.; Kidchob, T.; Gaspa, L.; Nicolini, C. Thermal stability of lysozyme Langmuir−Schaefer films by FTIR spectroscopy. *Langmuir* **2007**, *23* (3), 1147−1151.

(26) Kamerzell, T. J.; Middaugh, C. R. Two-dimensional correlation spectroscopy reveals coupled immunoglobulin regions of differential flexibility that influence stability. *Biochemistry* **2007**, *46* (34), 9762−9773.

(27) Zhao, H.; Jones, C. L.; Cowins, J. V. Lipase dissolution and stabilization in ether-functionalized ionic liquids. *Green Chem.* **2009**, *11*, 1128−1138. Baker, S. N.; McCleskey, T. M.; Pandey, S.; Baker, G. A. Fluorescence studies of protein thermostability in ionic liquid. *Chem. Commun.* **2004**, 940−941.

(28) Mandal, P. K.; Paul, A.; Samanta, A. Excitation wavelength dependent fluorescence behavior of the room temperature ionic liquids and dissolved dipolar solutes. *J. Photochem. Photobiol., A* **2006**, *182*, 113.

(29) Shu, Y.; Liu, M.; Chen, S.; Chen, X.; Wang, J. New insight into molecular interactions of imidazolium ionic liquids with bovine serum albumin. *J. Phys. Chem. B* **2011**, *115*, 12306−12314.

(30) Georlette, D.; Blaise, V.; Bouillenne, F.; Damien, F.; Thorbjarnardottir, S. H.; Depiereux, E.; Gerday, C.; Uversky, V. N.; Feller, G. Adenylation-dependent conformation and unfolding pathways of the NAD1-dependent DNA ligase from the thermophile *Thermus scotoductus*. *Biophys. J.* **2004**, *86*, 1089−1104.

(31) Meskers, S.; Ruysschaert, J. M.; Goormaghtigh, E. Hydrogen−deuterium exchange of streptavidin and its complex with biotin studied by 2D-attenuated total reflection fourier transform infrared spectroscopy. *J. Am. Chem. Soc.* **1999**, *121* (22), 5115−5122.

(32) Thakur, G.; Leblanc, R. M. Conformation of lysozyme langmuir monolayer studied by infrared reflection absorption spectroscopy. *Langmuir* **2009**, *25* (5), 2842−2849.
(33) Arrondo, J. L. R.; Muga, A.; Castresana, J.; Goni, F. M. Quantitative studies of the structure of proteins in solution by Fourier-transform infrared spectroscopy. *Prog. Biophys. Mol. Biol.* **1993**, *59* (1), 23−56.
(34) Schwartz, C. M.; M.Drown, P.; MacDonald, G. Difference FTIR studies reveal nitrogen-containing amino acid side chains are involved in the allosteric regulation of RecA. *Biochemistry* **2005**, *44* (28), 9733−9745.
(35) Nobilis, P.; Margaritifera, P. Soluble organic matrices of the calcitic prismatic shell layers of two Pteriomorphid bivalves. *J. Biol. Chem.* **2003**, *278* (17), 15168−15177.
(36) Butler, B. C.; Hanchett, R. H.; Rafailov, H.; MacDonald, G. Investigating structural changes induced by nucleotide binding to RecA using difference FTIR. *Biophys. J.* **2002**, *82* (4), 2198−2210.
(37) Dong, A.; Randolph, T. W.; Carpenter, J. F. Entrapping intermediates of thermal aggregation in $\acute{\alpha}$-helical proteins with low concentration of guanidine hydrochloride. *J. Biol. Chem.* **2000**, *275* (36), 27689−27693.
(38) Dupeyrat, F.; Vidaud, C.; Lorphelin, A.; Berthomieu, C. Long distance charge redistribution upon Cu,Zn-superoxide dismutase reduction: significance for dismutase function. *J. Biol. Chem.* **2004**, *279* (46), 48091−48101.
(39) Goormaghtigh, E.; Cabiaux, V.; Ruysschaert, J. M. Determination of soluble and membrane protein structure by Fourier transform infrared spectroscopy. III. Secondary structures. *Subcell Biochem.* **1994**, *23* (0), 405−450.
(40) Noda, I. Two-dimensional infrared spectroscopy. *J. Am. Chem. Soc.* **1989**, *111* (0), 8116−8118.
(41) Bartik, K.; Redfield, C.; Dobson, C. M. Measurement of the individual pK_a values of acidic residues of hen and turkey lysozymes by two-dimensional 1H NMR. *Biophys. J.* **1994**, *66* (4), 1180−1184.
(42) Mongan, J.; Case, D. A.; Mccammon, J. A. Accurate description of van der Waals complexes by density functional theory including empirical corrections. *J. Comput. Chem.* **2004**, *25* (12), 2039−2048.
(43) Sniegowski, J. A.; Lappe, J. W.; Patel, H. N.; Huffman, H. A.; Wachter, R. M. Base catalysis of chromophore formation in Arg^{96} and Glu^{222} variants of green fluorescent protein. *J. Biol. Chem.* **2005**, *280* (28), 26248−26255.
(44) Demchuk, E.; Wade, R. C. Improving the continuum dielectric approach to calculating pK_as of ionizable groups in proteins. *J. Phys. Chem.* **1996**, *100* (43), 17373−17387.
(45) Blake, C. C. F.; Johnson, L. N.; Mair, G. A.; North, A. C. T.; Phillips, D. C.; Sarma, V. R. Structure of hen egg-white lysozyme. A three-dimensional Fourier synthesis at 2.0 Å resolution. *Nature* **1965**, *206* (0), 757−761.
(46) Jolles, J.; Spotorno, G.; Jolles, Ñ. Lysozymes characterized in duck egg-white: Isolation of a histidine less lysozyme. *Nature* **1965**, *208* (5016), 1204−1205.
(47) Imoto, T.; Johnson, L. N.; North, A. C. T.; Phillips, D. C.; Rupley, J. A. In *The Enzymes*; Boyer, Ñ. D., Ed.; Academic Press, Inc.: New York, 1977; pp 665−868.
(48) Nielsen, J. E.; Mccammon, J. A. On the evaluation and optimization of protein X-ray structures for pK_a calculations. *Protein Sci.* **2003**, *12* (2), 313−326.
(49) Friess, S. D.; Zenobi, R. Protein structure information from mass spectrometry? Selective titration of arginine residues by sulfonates. *J. Am. Soc. Mass Spectrom.* **2001**, *12* (7), 810−818.